© 2017. Published by The Company of Biologists Ltd | Journal of Experimental Biology (2017) 220, 856-867 doi:10.1242/jeb.146845

RESEARCH ARTICLE

Evolution of vocal patterns: tuning hindbrain circuits during species divergence

Charlotte L. Barkan[1], Erik Zornik[2] and Darcy B. Kelley[1,3,*]

ABSTRACT

The neural circuits underlying divergent courtship behaviors of closely related species provide a framework for insight into the evolution of motor patterns. In frogs, male advertisement calls serve as unique species identifiers and females prefer conspecific to heterospecific calls. Advertisement calls of three relatively recently (~8.5 Mya) diverged species – *Xenopus laevis*, *X. petersii* and *X. victorianus* – include rapid trains of sound pulses (fast trills). We show that while fast trills are similar in pulse rate (~60 pulses s^{-1}) across the three species, they differ in call duration and period (time from the onset of one call to the onset of the following call). Previous studies of call production in *X. laevis* used an isolated brain preparation in which the laryngeal nerve produces compound action potentials that correspond to the advertisement call pattern (fictive calling). Here, we show that serotonin evokes fictive calling in *X. petersii* and *X. victorianus* as it does in *X. laevis*. As in *X. laevis*, fictive fast trill in *X. petersii* and *X. victorianus* is accompanied by an *N*-methyl-D-aspartate receptor-dependent local field potential wave in a rostral hindbrain nucleus, DTAM. Across the three species, wave duration and period are strongly correlated with species-specific fast trill duration and period, respectively. When DTAM is isolated from the more rostral forebrain and midbrain and/or more caudal laryngeal motor nucleus, the wave persists at species-typical durations and periods. Thus, intrinsic differences within DTAM could be responsible for the evolutionary divergence of call patterns across these related species.

KEY WORDS: Central pattern generator, Vocalization, Communication, *Xenopus*, Evolution, Motor

INTRODUCTION

The complex temporal dynamics of motor patterns arise from finely tuned circuits in the central nervous system. Differences in courtship behaviors between populations can contribute to pre-mating isolation and thus to speciation (Hoskin and Higgie, 2010). Within extant species of African clawed frogs (*Xenopus* and *Silurana*), males produce a species-specific advertisement call that coordinates courtship (Tobias et al., 2011). Differences in temporal features of advertisement calls can serve as species identifiers (Tobias et al., 2011). Female anurans, including *Xenopus laevis*, prefer conspecific to heterospecific advertisement calls (e.g. Ryan and Rand, 1993; Gerhardt, 1994; Picker, 1983). Thus, call divergence during speciation could contribute to prezygotic reproductive isolation, reinforcing the genetic divergence of populations and driving speciation. While the ultimate results of divergence in courtship signaling have been extensively examined (e.g. West-Eberhard, 1983; Kirkpatrick and Ryan, 1991; Gerhardt, 1994), specific changes in the neural circuits responsible for the evolution of signaling have only recently been identified (e.g. Chakraborty and Jarvis, 2015; Leininger and Kelley, 2015; Katz, 2016). Neural circuits controlling stereotyped courtship behaviors produced by closely related species can reveal these proximate mechanisms (Katz and Harris-Warrick, 1999).

Each species of *Xenopus* produces a distinct advertisement call consisting of a train of several sound pulses (Tobias et al., 2011; Leininger and Kelley, 2015). The *laevis* clade – *X. laevis sensu lato* – consists of four geographically separated species that diverged ~8.5 Mya (Furman et al., 2015; Evans et al., 2004; Fig. 1A), each with a distinctive advertisement call (Tobias et al., 2011; e.g. Fig. 1B–D). Because these species diverged relatively recently, the neural circuits producing these temporally distinct patterns are likely to be similar, allowing us to identify mechanisms for tuning specific temporal call features.

Xenopus vocal behavior and its underlying neural circuitry have been studied most extensively in *X. laevis* (reviewed in Zornik and Kelley, 2017). The male *X. laevis* advertisement call consists of highly stereotyped, alternating trains of fast and slow rate sound pulses (trills: see Fig. 1B). Compound action potentials (CAPs), produced by groups of hindbrain vocal motor neurons in the laryngeal motor nucleus IX-X (LMN), exit the central nervous system via the fourth rootlet of cranial nerve IX-X (laryngeal nerve) and travel to the vocal organ, the larynx, generating muscle contractions and sounds (Tobias and Kelley, 1987; Yager, 1992). The pattern of CAPs recorded from the laryngeal nerve of calling *X. laevis* males corresponds to the pattern of sound pulses during *in vivo* calling (Yamaguchi and Kelley, 2000). Fictive advertisement calling – CAP patterns that parallel *in vivo* call patterns – can be evoked by application of serotonin to the *in vitro* male brain (Fig. 2A; Rhodes et al., 2007), providing a powerful preparation for understanding the underlying neural circuits.

Using this preparation, a central pattern generator (CPG) located in the hindbrain was identified as responsible for fictive call patterns in *X. laevis* (Rhodes et al., 2007). The primary premotor nucleus in the CPG is DTAM (in earlier literature, an abbreviation for the dorsal tegmental area of the medulla, now used as a proper name), a putative homolog of the para-trigeminal respiratory group in lampreys and the parabrachial complex in mammals (see Discussion). DTAM projects to the caudal hindbrain LMN (Wetzel et al., 1985; Zornik and Kelley, 2007), homologous to the nucleus ambiguus of mammals (Albersheim-Carter et al., 2016), which also contributes to CPG function (Fig. 2A). Neurons in DTAM monosynaptically excite LMN motor neurons that produce vocal patterns (Zornik and Kelley, 2008; Yamaguchi et al., 2008; Zornik et al., 2010; Zornik and Yamaguchi,

[1]Doctoral Program in Neurobiology and Behavior, Columbia University, New York, NY 10032, USA. [2]Biology Department, Reed College, Portland, OR 97202, USA. [3]Department of Biological Sciences, Columbia University, New York, NY 10025, USA.

*Author for correspondence (dbk3@columbia.edu)

D.B.K., 0000-0003-4736-4939

Received 8 August 2016; Accepted 13 December 2016

Journal of Experimental Biology

Journal of Experimental Biology (2017) 220, 856-867 doi:10.1242/jeb.146845

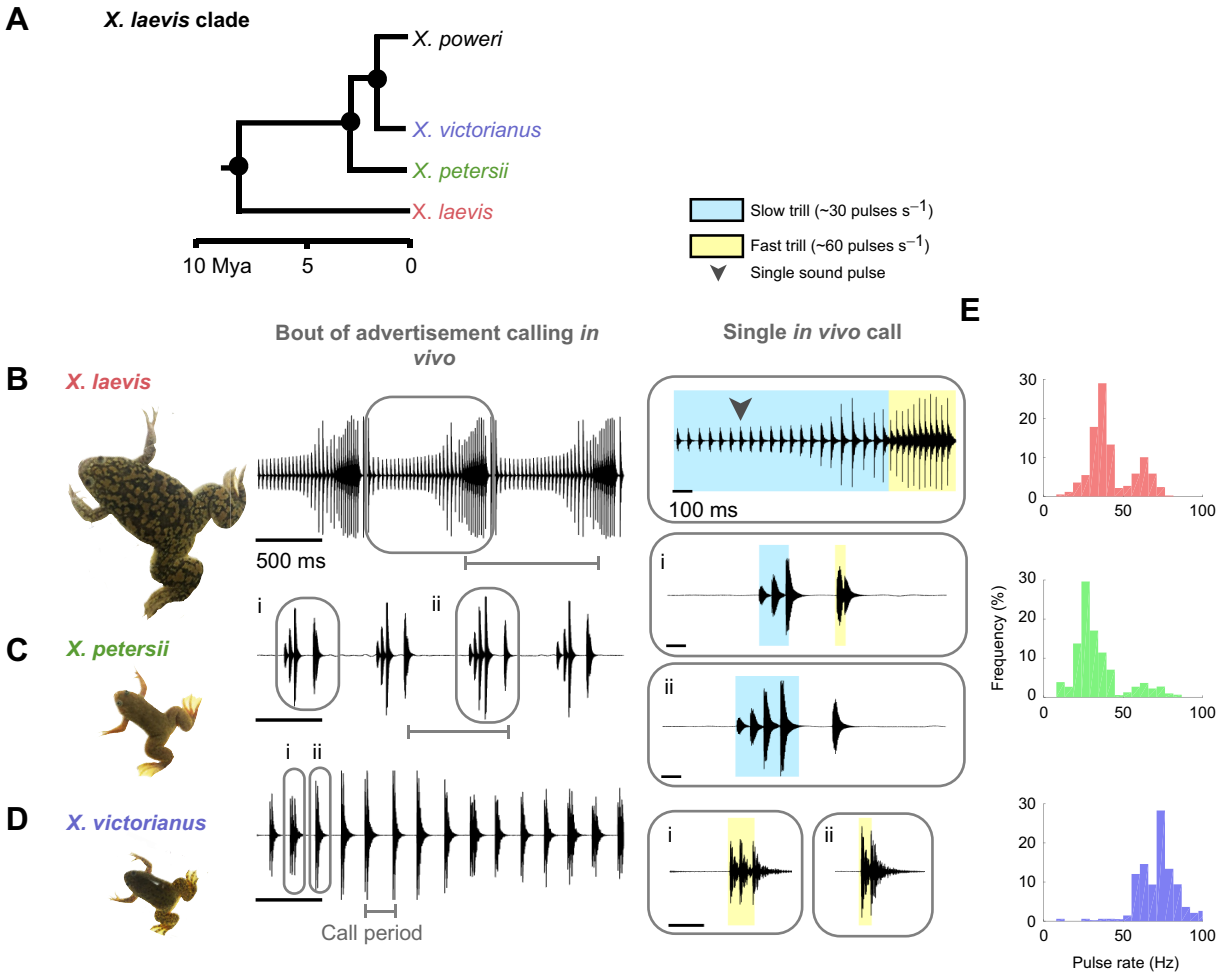

Fig. 1. Species-specific advertisement call patterns in the *Xenopus laevis* clade. (A) The *X. laevis* clade includes four species: *X. laevis*, *X. petersii*, *X. victorianus* and *X. poweri*, estimated to have diverged from their most recent common ancestor 8.5 Mya (Furman et al., 2015). (B–D) Representative male advertisement calls in *X. laevis*, *X. petersii* and *X. victorianus* consist of a series of sound pulses (trills) with characteristic temporal patterns and rates (Hz). (B) Oscillogram (intensity versus time) of the *X. laevis* biphasic advertisement call. The slow trill (~30 Hz, blue) alternates with the fast trill (~60 Hz, yellow). (C) Oscillogram of the biphasic *X. petersii* call. A short (i.e. 3–4 pulses) slow trill (blue) is followed by either (i) two fast pulses (yellow) or (ii) a single sound pulse. (D) Oscillogram of the monophasic *X. victorianus* call. The call consists of short trills with either (i) three or (ii) two fast pulses (yellow). (E) Frequency histograms depict pulse rate distribution for each species. In each species, a minimum is present at ~50 Hz, separating fast trill and slow trill rates.

2012). A local field potential (LFP) wave recorded from DTAM coincides with fast trill and is NMDA receptor dependent (Zornik et al., 2010). Taken together, available evidence suggests that in *X. laevis*, DTAM neurons drive the LFP wave and control call duration and period (Zornik and Yamaguchi, 2012).

What mechanisms underlie vocal divergence in the *laevis* clade? While all species in the clade produce fast trills, the duration and period (time from the onset of one call to the onset of the following call) of their calls differ substantially (Tobias et al., 2011). We used the *in vitro* brain preparation originally developed in *X. laevis* (Rhodes et al., 2007) to compare motor and premotor activity during fictive calling in *X. laevis*, *X. petersii* and *X. victorianus*. In this study, we tested the hypothesis that species-specific tuning of the DTAM circuitry underlies call divergence in the *laevis* clade.

MATERIALS AND METHODS

Procedures

Animals

All animal care and experimental procedures conformed to guidelines set forth by the National Institutes of Health and were approved by Columbia University's Institutional Animal Care and Use guidelines (protocol no. AC-AAM1051). Sexually mature male *X. laevis* (mean±s.d. mass: 34.5±6.0 g, n=10), *X. petersii* (11.9±0.7 g, n=10) and *X. victorianus* (11.2±1.2 g, n=5) were used in experiments. Animals were raised in the laboratory colony or purchased from Xenopus Express (Brooksville, FL, USA), group housed in polycarbonate tanks, each with 10 l of filtered water changed twice weekly following feeding with frog brittle (Xenopus Express), and kept on a 12 h light:12 h dark schedule at 20°C (*X. laevis*) or 23°C (*X. petersii* and *X. victorianus*).

Vocalization recordings

Male frogs (n=5 each for *X. laevis*, *X. petersii* and *X. victorianus*) were injected via the dorsal lymph sac with 200 µmol l^{-1} human chorionic gonadotropin 48 and 24 h before calls were recorded. Each frog was placed in a glass aquarium (60×15×30 cm, water depth 25 cm, temperature 20–22°C) in a room illuminated dimly with red light. After 10 min of habituation, a conspecific female was placed in the tank for 30–45 min or overnight during a sound-activated recording (Audacity®, http://www.audacityteam.org/). Vocalizations were recorded with a hydrophone (CA30 or H2a, Aquarian Audio Products, Shoreline, WA, USA); the signal was

Journal of Experimental Biology (2017) 220, 856-867 doi:10.1242/jeb.146845

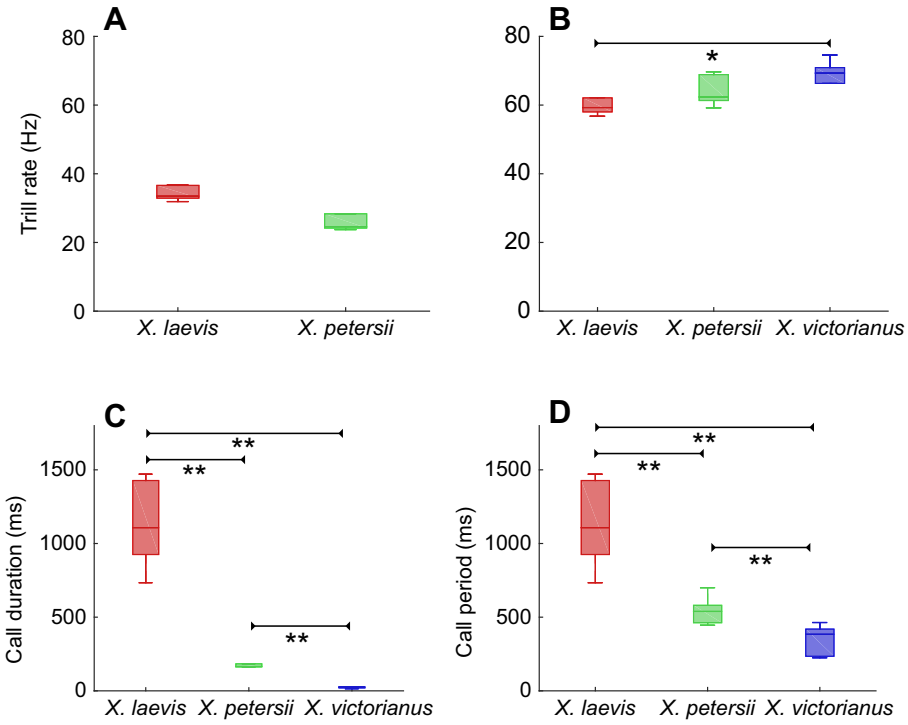

Fig. 2. Comparison of the temporal features of *in vivo* calling. Boxplots illustrate the 25th and 75th percentiles; the horizontal line is the median, whiskers were calculated using Tukey's method and depict the most extreme data value that is not an outlier. Red indicates *X. laevis* (*in vivo* n=5), green *X. petersii* (*in vivo* n=5) and blue *X. victorianus* (*in vivo* n=5). *P<0.01, **P<0.0001 [generalized linear models (GLMs) with gamma distribution]. (A) Slow pulse rates of *in vivo* calls do not differ significantly between *X. laevis* and *X. petersii* (P>0.05). (B) Fast pulse rates of *in vivo* calls do not differ significantly between *X. laevis* and *X. petersii* (P>0.05) or between *X. victorianus* and *X. petersii* (P>0.05). *Xenopus laevis* fast rate is significantly slower than that of *X. victorianus*. (C) Call duration differs significantly between all species. (D) Call period differs significantly between all species.

digitized (Omega SV, Lexicon Pro), and saved to a personal computer in .wav format (Amadeus Pro, HairerSoft, Kenilworth, UK or Audacity®).

In vitro brain preparation

Male frogs (*X. laevis* n=12, *X. petersii* n=14, *X. victorianus* n=5) were deeply anesthetized by injection of 1.3% tricaine methanesulfonate (MS-222, Sigma; *X. laevis*: 500–700 µl, *X. petersii* and *X. victorianus*: 200 µl) into the dorsal lymph sac and brains were removed from the cranium in ice-cold saline (in mmol l^{-1}: 96 NaCl, 20 $NaHCO_3$, 2 $CaCl_2$, 2 KCl, 0.5 $MgCl_2$, 10 Hepes and 11 glucose, pH 7.8, oxygenated with 99% O_2). Following recovery for 1 h in saline at room temperature, the brains were pinned in a silicone elastomer-lined recording dish (Sylgard, Dow Corning, Midland, MI, USA) and constantly superfused with fresh oxygenated saline at room temperature. CAPs were recorded with an extracellular suction electrode placed on the posterior rootlet of cranial nerve IX-X (laryngeal nerve) that contains the axons of the laryngeal motor neurons (Simpson et al., 1986). To elicit a fictive motor pattern on the laryngeal nerve, serotonin (Sigma) was bath applied to the recording dish to a final concentration of 30 or 60 µmol l^{-1} (Zornik and Yamaguchi, 2012). The signal from the nerve was amplified ×1000 (Model 1700, A-M Systems, Carlsborg, WA, USA) and band-pass filtered (10 Hz to 5 kHz), digitized at 10 or 20 kHz (Digidata 1400A, Molecular Devices, Sunnyvale, CA, USA), and recorded on a personal computer. After 5 min of application, serotonin was washed out by reinstating saline superfusion. Serotonin was then re-applied every 60 min for the next 4–8 h.

LFPs in DTAM were recorded using a low-impedance carbon fiber extracellular electrode (300–500 kΩ, Kation Scientific, Minneapolis, MN, USA) while simultaneously recording activity in the laryngeal nerve. The signal was amplified ×100, digitized at 10 or 20 kHz and bandpass filtered at 0.1 Hz to 10 kHz. Either the pia covering the cerebellum was removed to allow the DTAM electrode to penetrate or the cerebellum and tectum were transected sagittally at the midline, reflected laterally to expose DTAM, and pinned. The DTAM electrode was placed ∼100 µm posterior to the tectum–cerebellum border, ∼200 µm from the lateral edge of the fourth ventricle and ∼650 µm below the pial surface. Five *X. laevis*, five *X. petersii* and two *X. victorianus* brains were transected in the transverse plane, caudal to the laryngeal nerve, to isolate DTAM from the LMN. Two *X. laevis* brains and three *X. petersii* brains were transected in the transverse plane just rostral to DTAM, in addition to the caudal transection, to also remove any descending inputs from the midbrain and forebrain.

Pharmacology

In one *X. laevis* brain (to confirm previous findings: Zornik et al., 2010), three *X. petersii* brains and two *X. victorianus* brains, a selective NMDA antagonist, DL-2-amino-5-phosphonopentanoic acid (APV, Sigma), was bath applied to the recording dish at concentrations of 100–500 µmol l^{-1}. Changes in the LFP wave in response to drug application were recorded in DTAM and fictive calling was monitored via the laryngeal nerve suction electrode. After 5 min of APV application, 30 or 60 µmol l^{-1} serotonin was added to the bath for 10 min. One hour after the reinitiation of saline superfusion, serotonin was applied alone to determine whether the effect of APV was reversible.

Analyses

Calls

Calls were sampled from five males of each species. A single call (Fig. 1B–D) is the smallest vocal unit containing a characteristic and repeating pattern of sound pulses (Tobias et al., 2011). For all species, samples were randomly selected from continuous bouts of calling and lasted a minimum of 10 s and a maximum of 30 s. Samples contained a minimum of 15 calls and 100 pulses for each animal. Pulses were detected and analyzed using custom-written MATLAB scripts (MathWorks, Natick, MA, USA; all MATLAB scripts are available upon request from C.L.B.). Pulse rates ranging from 0 to 100 Hz were assigned to frequency bins (2 Hz width) and

Journal of Experimental Biology (2017) 220, 856-867 doi:10.1242/jeb.146845

then analyzed to determine the threshold rate for fast trill. Rate histograms revealed a minimum at ∼50 Hz in all three species (Fig. 1E) and thus 50 Hz was selected as the threshold for fast trill. In all species, slow trill onset was defined as two or more successive pulses with an instantaneous pulse rate <50 Hz (20 ms) and >10 Hz (100 ms). Fast trills followed slow trills. Fast trills with two or more successive pulses had a pulse rate >50 Hz (20 ms) and <100 Hz (10 ms). Call duration was measured from call onset to call offset. Call period was measured from the onset of a call to the onset of the following call.

In vitro brain analysis

Fictive vocal CAP patterns produced following serotonin application were collected and analyzed (*X. laevis* n=5, *X. petersii* n=6, *X. victorianus* n=3) using custom-written MATLAB scripts. For all species, samples were randomly selected from continuous bouts of fictive calling and lasted a minimum of 20 s and a maximum of 30 s. Samples contained a minimum of 15 calls and 100 pulses for each animal. Instantaneous CAP rate was calculated as the reciprocal of the time interval between two successive CAPs. As for *in vivo* calls, fictive slow trills followed fictive fast trills and typically consisted of a series of two or more pulses with an instantaneous pulse rate <50 Hz and >10 Hz. Fictive fast trills consisted of a series of two or more CAPs >50 Hz and <100 Hz. Fictive call duration was measured from fictive call onset to call offset. Fictive call period was measured from the onset of a fictive call to the onset of the following call.

The DTAM LFP was low-pass filtered to reveal a wave corresponding to fictive fast trill. Because the 5 Hz low-pass filter used for *X. laevis* does not accurately identify wave onset in species with shorter calls, a 20 Hz filter was used for *X. petersii* and *X. victorianus*. Wave onset was defined as the first peak in the second derivative of the low-pass filtered signal prior to the wave peak. Wave offset was defined as the first peak in the second derivative of the low-pass filtered signal following the wave peak. Onset and offset were visually confirmed and manually adjusted if necessary. Call and wave durations were measured from onset to offset time. Call and wave periods were measured from one call onset time to the onset of the following call.

Evoking fictive calling from the isolated brain requires the preservation of laryngeal nerve connections to the LMN during dissection, an intact hindbrain and effective oxygenation to preserve neural function. The success rate for these experiments is variable and can be low. Because the availability of mature male *X. victorianus* was extremely limited, fictive calling data points are reported individually in cases where n<5.

Statistics

Statistical analyses were carried out using MATLAB and R (R Core Team, Vienna, Austria). Because the data were not normally distributed, but the coefficient of variance was roughly constant across groups, generalized linear models (GLMs) with gamma distributions were used to compare *in vivo* and *in vitro* call characteristics across species (fast trill rate, slow trill rate, call duration and call period). Linear regression models were used to compare *in vivo* fast trill duration and period with *in vitro* fast trill duration and period, respectively. To compare the relationship between the onset and offset of the DTAM LFP with fast trill, the median for each species was used. A GLM was used to compare animal means for DTAM LFP wave duration and period in intact brains and for transected brains between *X. laevis* and *X. petersii*.

RESULTS

Advertisement calls across species

We recorded advertisement calls from five adult male *X. laevis*, *X. petersii* and *X. victorianus*. All three species produce a distinctive male advertisement call consisting of repeated trains of sound pulses or trills (Fig. 1B–D, Table 1). *Xenopus laevis* calls alternate between a slow trill (∼30 Hz) of ∼25 sound pulses and a fast trill (∼60 Hz) of ∼12 pulses (Fig. 1B). Similarly, *X. petersii* calls (Fig. 1C) consist of a slow trill with ∼3 pulses followed by a fast trill made up of 2 pulses (Fig. 1Ci, percentage of fast trills that are doublets: 35.2±26.2%, mean±s.d.) or a single pulse (Fig. 1Cii, identified as following a slow trill). The advertisement call of *X. victorianus*, however, consists of only fast trills made up of 3 or 2 pulses (Fig. 1Di,ii); slow trills are absent. Fast trills thus occur in all three species.

Species share similar trill rates

We used GLMs to compare vocal characteristics of advertisement calls across all three species (Fig. 2, Table 1). Slow trill pulse rates (Fig. 2A, Table 1) did not differ significantly between *X. laevis* and *X. petersii* (P>0.05; *X. victorianus* does not have a slow trill). Fast trill pulse rates did not differ significantly between *X. laevis* and *X. petersii* or between *X. petersii* and *X. victorianus* (P>0.05 for each comparison; Fig. 2B, Table 1). Fast trill rate was significantly faster in *X. victorianus* compared with *X. laevis* (P<0.01).

Call duration and period differ across species

Call duration (P<0.0001 for all comparisons; Fig. 2C, Table 1) and period (P<0.0001 for all comparisons; Fig. 2D, Table 1) differed significantly between all three species, with *X. laevis* having the longest call duration and period and *X. petersii* having the shortest call duration and period.

Serotonin induces fictive calling by the isolated *in vitro* brain

When the *X. laevis* brain was removed and placed in an oxygenated saline solution (Fig. 3A), bath application of serotonin resulted in species-specific activity patterns recorded from the laryngeal nerve (Fig. 3B–D). In male *X. laevis*, the temporal features of these *in vitro* CAPs parallel the pattern of sound pulses in the *in vivo*

Table 1. Comparison of *in vivo* and *in vitro* call characteristics of *Xenopus* species

Species	Fast pulse rate (Hz)	Fast CAP rate (Hz)*	Slow pulse rate (Hz)	Slow CAP rate (Hz)	*In vivo* call duration (ms)	*In vitro* call duration (ms)*	*In vivo* call period (ms)	*In vitro* call period (ms)*
X. laevis	59.7±2.3	58.5±4.5	27.7±0.7	31.1±3.3	1142.9±305.1	1273.1±303.0	1142.9±305.1	1260.0±297.7
X. petersii	64.4±4.5	61.3±6.2	26.8±4.7	29.3±0.36	178.2±30.7	177.2±86.4	538.7±99.6	683.4±225.5
X. victorianus	68.2±5.8	63.9±5.4 (58.0, 65.8, 68.3)	N/A	N/A	23.0±5.1	32.6±9.9 (44.1, 27.1, 26.7)	343.0±105.8	391.5±9.1 (381.1, 396.0, 397.7)

Data are means±s.d. *Individual values for *X. victorianus* are given in parentheses. Sample sizes: *X. laevis in vivo* n=5, *in vitro* n=5; *X. petersii in vivo* n=5, *in vitro* n=6; *X. victorianus in vivo* n=5, *in vitro* n=3.
CAP, compound action potential.

Journal of Experimental Biology (2017) 220, 856-867 doi:10.1242/jeb.146845

advertisement call (compare Fig. 1B with Fig. 3B) and have thus been termed fictive advertisement calling (Rhodes et al., 2007). If fundamental neural circuit properties for calling are conserved across the *X. laevis* clade, we hypothesized that serotonin should also elicit fictive advertisement calling in *X. petersii* and *X. victorianus*.

We found that bath application of serotonin to isolated brains also elicited patterned laryngeal nerve CAPs in *X. petersii* (n=6) and *X. victorianus* (n=3, due to limited availability of adult males of this species; Fig. 3C,D). As in *X. laevis* (n=5; Fig. 3B), these CAP patterns closely resembled the patterns of each species' advertisement call (compare Fig. 1 with Fig. 3). CAPs were produced at fast (~60 Hz; Fig. 3, yellow) and slow (~30 Hz: Fig. 3, blue) rates in *X. laevis* and *X. petersii*; *X. victorianus* brains produced only fast CAPs. Four of the six *X. petersii* brains produced slow trill CAPs and all produced fast trill CAPs. We conclude that

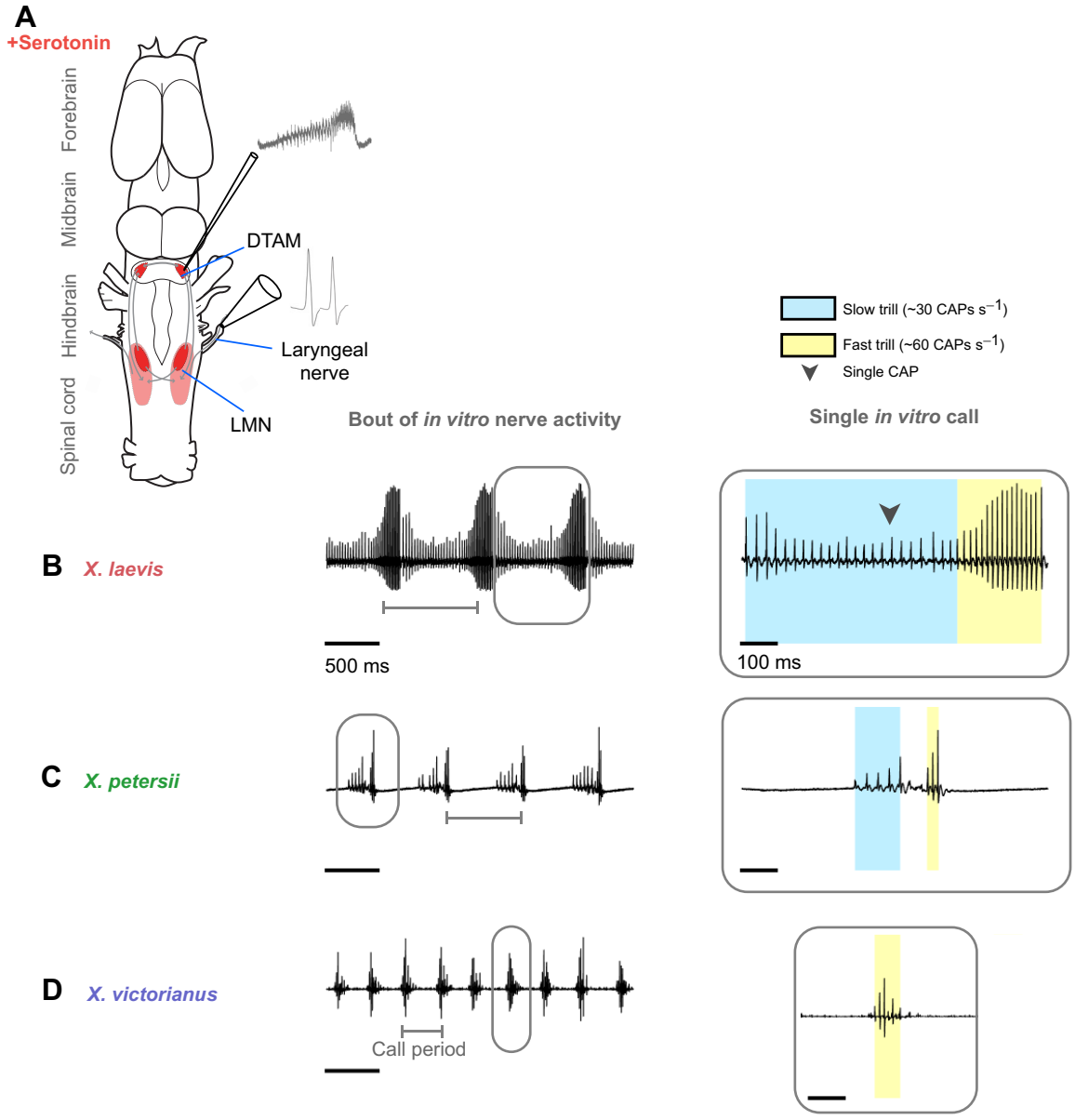

Fig. 3. Serotonin application to the *in vitro* brain induces patterned laryngeal nerve activity across species. (A) A schematic view of the isolated male hindbrain viewed from the dorsal surface; anterior is up. (B–D) In response to serotonin bath application, patterned bouts of activity – compound action potentials (CAPs) – produced by vocal motor neurons in the laryngeal motor nucleus (LMN), can be recorded from the laryngeal nerve. *In vitro* patterns correspond to advertisement call patterns (Fig. 1) and are termed fictive calls. During the fast trill of a fictive call, a local field potential (LFP) can be recorded from nucleus DTAM of the rostral hindbrain. Laryngeal motor neurons are located in the posterior LMN (pink) and project to the larynx via the laryngeal nerve (4th root of cranial nerve IX-X). Interneurons in the anterior LMN (red) project to the LMN and DTAM. DTAM interneurons (red) provide monosynaptic, excitatory input to laryngeal motor neurons. Axons from DTAM cross the midline to innervate the contralateral DTAM. (B–D) Left: representative laryngeal nerve activity bouts in *X. laevis*, *X. petersii* and *X. victorianus* following bath application of serotonin to the isolated brain. Right: single fictive calls with individually labeled slow (blue) and fast (yellow) trills. (B) Bouts of activity recorded from the *X. laevis* laryngeal nerve include alternating slow and fast CAPs. (C) Bouts of activity recorded from the *X. petersii* laryngeal nerve also include alternating slow and fast CAPs; call duration and period are shorter than in *X. laevis*. (D) The *in vitro* laryngeal nerve activity pattern produced by *X. victorianus* includes only fast CAPs.

Journal of Experimental Biology

Journal of Experimental Biology (2017) 220, 856-867 doi:10.1242/jeb.146845

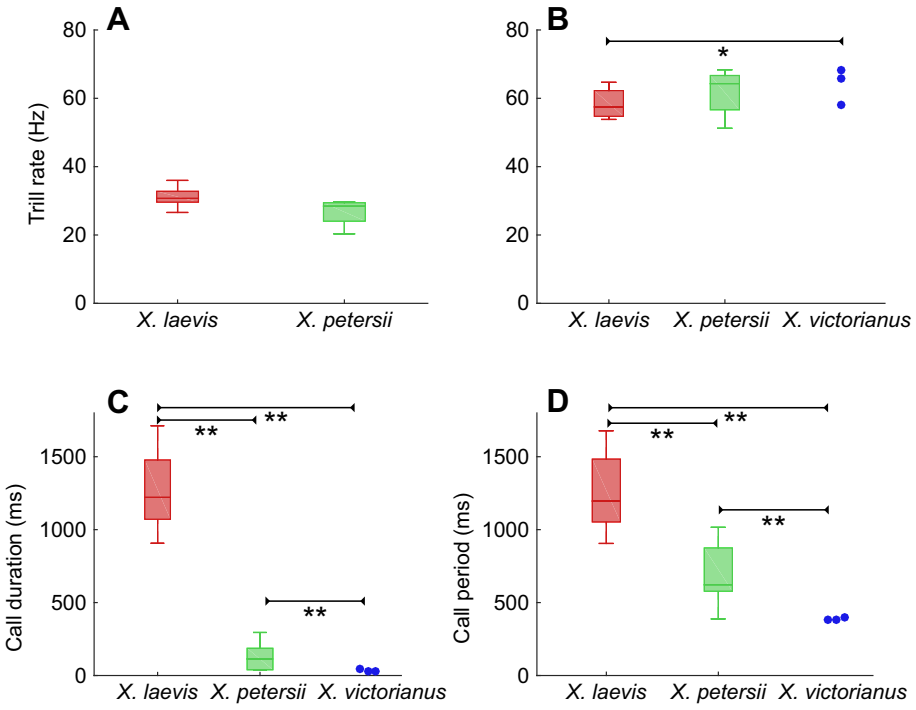

Fig. 4. Comparison of the temporal features of *in vitro* laryngeal nerve activity. Boxplots illustrate the 25th and 75th percentiles; the horizontal line is the median, whiskers were calculated using Tukey's method and depict the most extreme data value that is not an outlier. Red indicates *X. laevis* (*in vitro* n=5), green *X. petersii* (*in vitro* n=6) and blue *X. victorianus* (*in vitro* n=3). *P<0.01, **P<0.0001 (GLMs with gamma distribution). (A) Slow pulse rates of *in vivo* calls do not differ significantly between *X. laevis* and *X. petersii* (P>0.05). (B) Fast pulse rates of *in vivo* calls do not differ significantly between *X. laevis* and *X. petersii* (P>0.05) or between *X. victorianus* and *X. petersii* (P>0.05). *Xenopus laevis* fast rate is significantly slower than that of *X. victorianus*. (C) Call duration differs significantly between all species. (D) Call period differs significantly between all species.

fictive calling elicited by serotonin is a fundamental neural circuit property conserved across these three species.

Species share similar fictive trill rates

We used GLMs to compare characteristics of *in vitro* laryngeal nerve activity across all three species (Fig. 4, Table 1). Slow trill CAP rates (Fig. 4A, Table 1) did not differ significantly between *X. laevis* and *X. petersii* (P>0.05; *X. victorianus* does not have a slow trill). Fast trill CAP rates did not differ significantly between *X. laevis* and *X. petersii* or between *X. petersii* and *X. victorianus* (P>0.05 for each comparison; Fig. 4B, Table 1). Although fairly similar, fast trill rate was somewhat faster in *X. victorianus* than in *X. laevis* (P<0.01).

Fictive call duration and period differ across species

Fictive call duration (P<0.0001 for all comparisons; Fig. 4C, Table 1) and period (P<0.0001 for all comparisons; Fig. 4D, Table 1) differed significantly between all three species, with *X. laevis* having the longest fictive call duration and period and *X. petersii* having the shortest fictive call duration and period.

In vitro laryngeal nerve activity does not differ from *in vivo* advertisement calls

GLM analyses comparing fictive calling in the *in vitro* preparation with *in vivo* calling found no significant effects for fast rate, slow rate, call duration or call period. We conclude that fictive calling elicited by serotonin *in vitro* corresponds to *in vivo* calling in all three species.

A LFP wave in the premotor DTAM during fictive fast trill

We recorded DTAM activity during *in vitro* fictive calling in *X. laevis* (n=5), *X. petersii* (n=6) and *X. victorianus* (n=2). A LFP wave in DTAM (Fig. 5A) was associated with fictive fast trill (Fig. 5B) in all three species. This wave began before fictive fast trill (median±s.d. difference: *X. laevis*: −160.0±115.8 ms, *X. petersii*: −59.2±13.6 ms, *X. victorianus*: −47.6±10.0 ms) and terminated after fictive fast trill (median±s.d. difference: *X. laevis*: 106.7±73.4 ms, *X. petersii*: 49.4±8.3 ms, *X. victorianus*: 28.3±12.2 ms) (Fig. 5C).

Because *in vivo* and *in vitro* call durations and periods were significantly longer in *X. laevis* than in *X. petersii* and *X. victorianus* (above, Fig. 4D,E), and the DTAM LFP coincides closely with fast trill in each species, we examined the relationship between the duration and period of the LFP wave and the duration and period of fictive fast trill using linear regression in pooled individuals of all three species (*X. laevis* n=5, *X. petersii* n=6, *X. victorianus* n=2). Wave duration was linearly (Fig. 5D) and strongly (R^2=0.947, slope=0.6618, P<0.0001) related to fictive fast trill duration. Wave periods in all three species were also linearly (Fig. 5E) and strongly (R^2=0.991, slope=1.0028, P<0.0001) related to periods between successive fast trills. We conclude that the temporal relationship of the DTAM LFP to fictive fast call duration and period is conserved across the three species.

In *X. laevis*, fictive fast trills and the DTAM LFP wave are both NMDA dependent (Zornik et al., 2010). We hypothesized that if similar mechanisms underlie calling in *X. petersii* and *X. victorianus*, as is suggested by the similarities in the underlying DTAM activity, calling would be NMDA dependent in all species examined here. We thus applied APV (a competitive NMDA receptor antagonist) to fictively singing brains in *X. laevis* (n=1, to confirm previous findings; see Zornik et al., 2010), *X. petersii* (n=3) and *X. victorianus* (n=2) to determine whether NMDA receptor dependence is conserved. One hour prior to APV application, all preparations produced fictive calling accompanied by a LFP wave in DTAM (Fig. 6A) in response to serotonin application. Pretreatment for 15 min with APV blocked both fictive calling and the LFP wave in response to serotonin (Fig. 6B). An hour after APV washout, serotonin-induced fictive calling and the DTAM wave returned (Fig. 6C). The NMDA dependence of the DTAM wave is thus conserved within the *laevis* clade.

LFP wave generation appears autonomous to DTAM

Next, we set out to determine whether DTAM alone is responsible for generating the LFP wave, rather than other components

Journal of Experimental Biology (2017) 220, 856-867 doi:10.1242/jeb.146845

of the vocal circuit, such as interneurons located in the anterior portion of the LMN (red portion of LMN, Fig. 2A). These neurons innervate DTAM (Zornik and Kelley, 2007), raising the possibility that the LMN controls the timing of the LFP wave. To address this question, we transected the *in vitro* brain between DTAM and the LMN, just caudal to the laryngeal nerve. After transection, serotonin application produced a DTAM LFP wave that closely resembled the DTAM LFP wave produced by intact brains in *X. laevis* (n=5), *X. petersii* (n=5) and *X. victorianus* (n=2) (Fig. 7A,B). We used GLMs to examine wave duration and period across species and

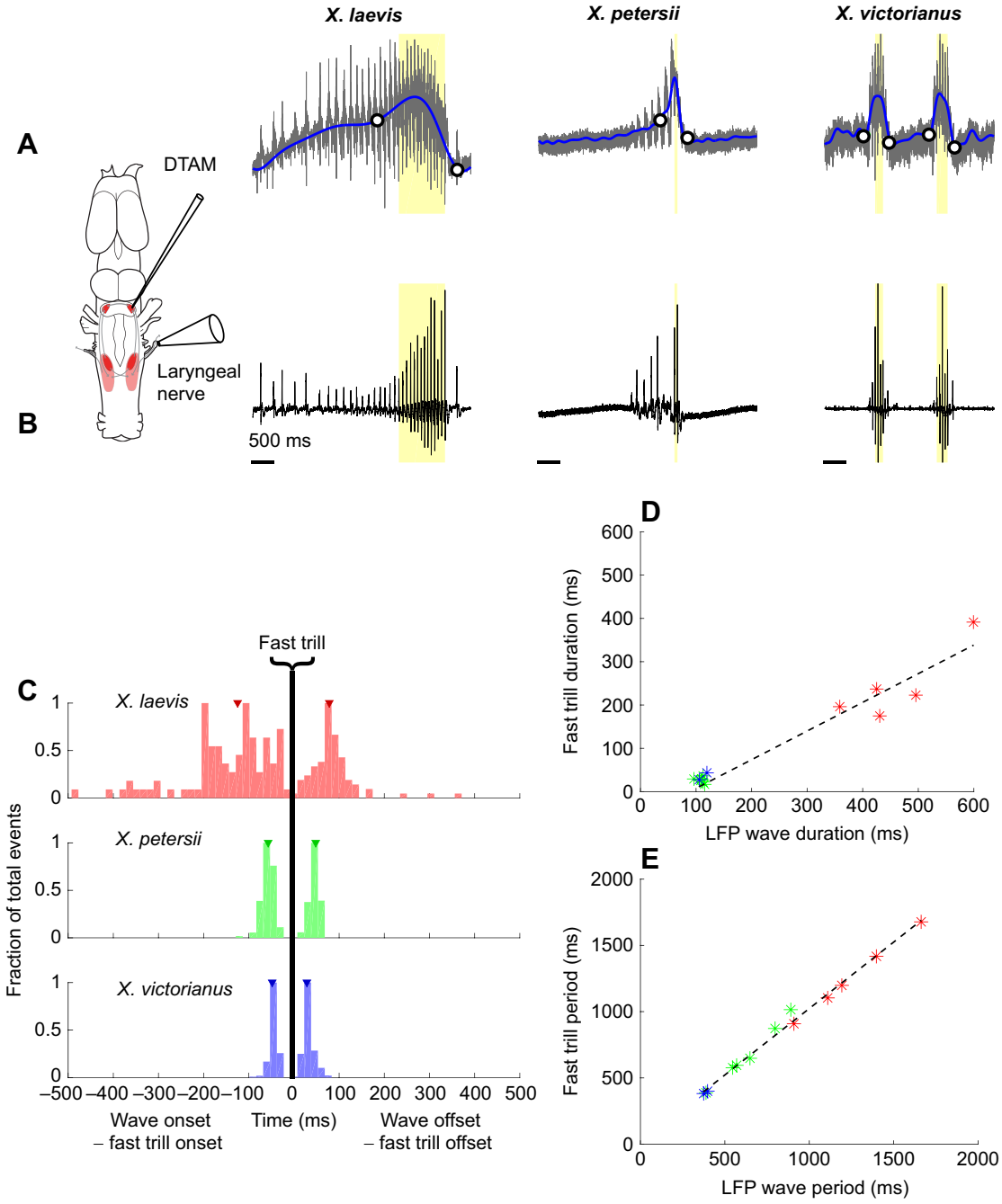

Fig. 5. A LFP wave in DTAM corresponds to fast trill in all species. (A) Representative extracellular recording in DTAM (gray) and resulting LFP wave [blue, low-pass filtered at 5 Hz for *X. laevis* (n=5) and 20 Hz for *X. petersii* (n=6) and *X. victorianus* (n=2)] in response to serotonin application coincides with the fast trill (yellow) of the (B) fictive call simultaneously recorded from the laryngeal nerve (black). Wave onset and offset are depicted by open circles. (C) The DTAM LFP begins before the start of each fast trill and ends after the trill stops. The fast trill onset is subtracted from the corresponding wave onset, resulting in a negative number across species (median±s.d.: *X. laevis*: −160.0±115.8 ms, *X. petersii*: −59.2±13.6 ms, *X. victorianus*: −47.6±10.0 ms). The fast trill offset is subtracted from the wave offset, resulting in a positive value across species (*X. laevis*: 106.7±73.4 ms after, *X. petersii*: 49.4±8.3 ms, *X. victorianus*: 28.3±12.2 ms). The *y*-axis bins are percentage of total events and arrowheads indicate group medians. (D) Linear regression analysis of mean fictive fast trill duration versus each animal's corresponding mean DTAM LFP wave duration. Asterisks depict mean values of individual animals (R^2=0.947, slope=0.6618, P<0.0001). (E) Linear regression analysis of inter-call period versus each animal's corresponding wave period. Asterisks depict mean values of individual animals (R^2=0.991, slope=1.0028, P<0.0001).

Journal of Experimental Biology (2017) 220, 856-867 doi:10.1242/jeb.146845

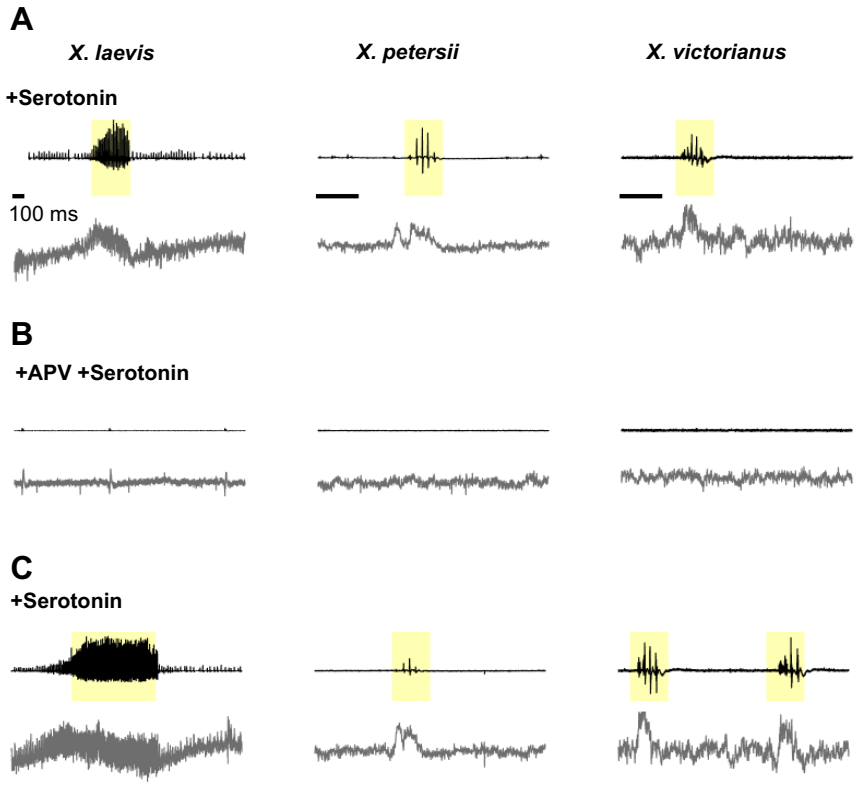

Fig. 6. The DTAM LFP wave is NMDA dependent. (A) Representative laryngeal nerve (black, top) and DTAM recordings (bottom, gray) following serotonin application *in vitro* in *X. laevis* (*n*=1), *X. petersii* (*n*=3) and *X. victorianus* (*n*=2). Fast trill is highlighted in yellow. (B) Laryngeal nerve (top) and DTAM (bottom) activity are abolished by 500 µmol l^{-1} APV added 15 min prior to serotonin application. (C) Laryngeal nerve (top) and DTAM (bottom) activity are restored following 1 h washout and re-application of serotonin.

found that both were significantly longer in *X. laevis* than in *X. petersii* and *X. victorianus* (Fig. 7C,D, $P<0.0001$ for all comparisons). *Xenopus petersii* wave period ($P<0.0001$) but not duration ($P>0.05$) was significantly longer than that of *X. victorianus*. Transections did not significantly alter wave duration in *X. laevis*, *X. petersii* or *X. victorianus* ($P>0.05$, means±s.d.: *X. laevis*: 444.2±29.6 ms intact, 465.3±28.9 ms transected; *X. petersii*: 108.7±7.3 ms intact, 118.0±2.3 ms transected; *X. victorianus* individual means: 119.8 and 105.4 ms intact, 113.2 and 121.1 ms transected; Fig. 7C). Wave periods in all species were also unaffected by transection ($P>0.05$, means±s.d.: *X. laevis*: 1115.6±188.8 ms intact, 1016.2±71.4 ms transected; *X. petersii*: 695.7±157.5 ms intact, 733.9±194.4 ms transected; *X. victorianus* individual values: 372.9 and 396.6 ms intact, 442.5 and 463.3 ms transected; Fig. 7D). We conclude that the duration and the period of the DTAM LFP wave do not reflect inputs from the LMN in these three species.

DTAM also receives input from the central amygdala located in the ventral forebrain (Brahic and Kelley, 2003; Hall et al., 2013). Because previous work has also shown that removal of the midbrain and forebrain does not disrupt fictive calling in *X. laevis* (Yu and Yamaguchi, 2010), we predicted that species-specific LFP wave patterns are generated autonomously within the hindbrain compartment that includes DTAM. To test this prediction, we combined a transection that eliminated LMN inputs with an additional transection just anterior to the cerebellum that removed inputs from the midbrain and forebrain in two *X. laevis* and three *X. petersii* brains. We found that following both transections, the LFP waves persisted in response to serotonin application (wave duration: *X. laevis*: 395.5, 334.3 ms, *X. petersii*: 141.5, 166.5, 130.4 ms; wave period: *X. laevis*: 1212.7, 1092.6 ms, *X. petersii*: 724.2, 1024.0, 662.1 ms; compare with values above for intact and transected animals). We incorporated these values into our GLMs for wave duration and period and found no significant effect of this anterior transection ($P>0.05$ for each GLM). These more limited observations suggest that DTAM LFP wave parameters also do not reflect inputs from midbrain or forebrain in the *X. laevis* clade, reinforcing the idea that intrinsic features of the DTAM LFP govern species differences in vocal patterns.

DISCUSSION

Divergent temporal features of songs are supported by shared neural circuit elements

Three relatively recently (8.5Mya) diverged species within the *laevis* clade – *X. laevis*, *X. petersii* and *X. victorianus* (Furman et al., 2015) – produce male advertisement calls with distinct temporal properties (Tobias et al., 2011). All of these species produce advertisement calls that include fast trills, but call duration and period are significantly different across all three species, with *X. laevis* having the longest call duration and period and *X. victorianus* having the shortest. We show here that key features of the neural circuitry responsible for vocal patterning are conserved across these species. Species-specific fictive advertisement calls (*in vitro* nerve activity patterns that parallel *in vivo* sound pulse patterns) can be elicited by applying serotonin to the isolated brain in each species. However, as is the case for actual advertisement calls recorded *in vivo*, fictive call duration and period recorded *in vitro* vary significantly across species.

Next, we examined premotor activity that might be responsible for species differences in call duration and period. In each species, fictive fast trills coincide with a LFP wave recorded from the rostral hindbrain nucleus DTAM. Wave duration and period are tightly correlated with fictive fast trill duration and period across individuals of each species. Furthermore, the LFP wave is NMDA receptor dependent in all species. Collectively, these findings support conserved involvement of NMDA-dependent DTAM

Journal of Experimental Biology (2017) 220, 856-867 doi:10.1242/jeb.146845

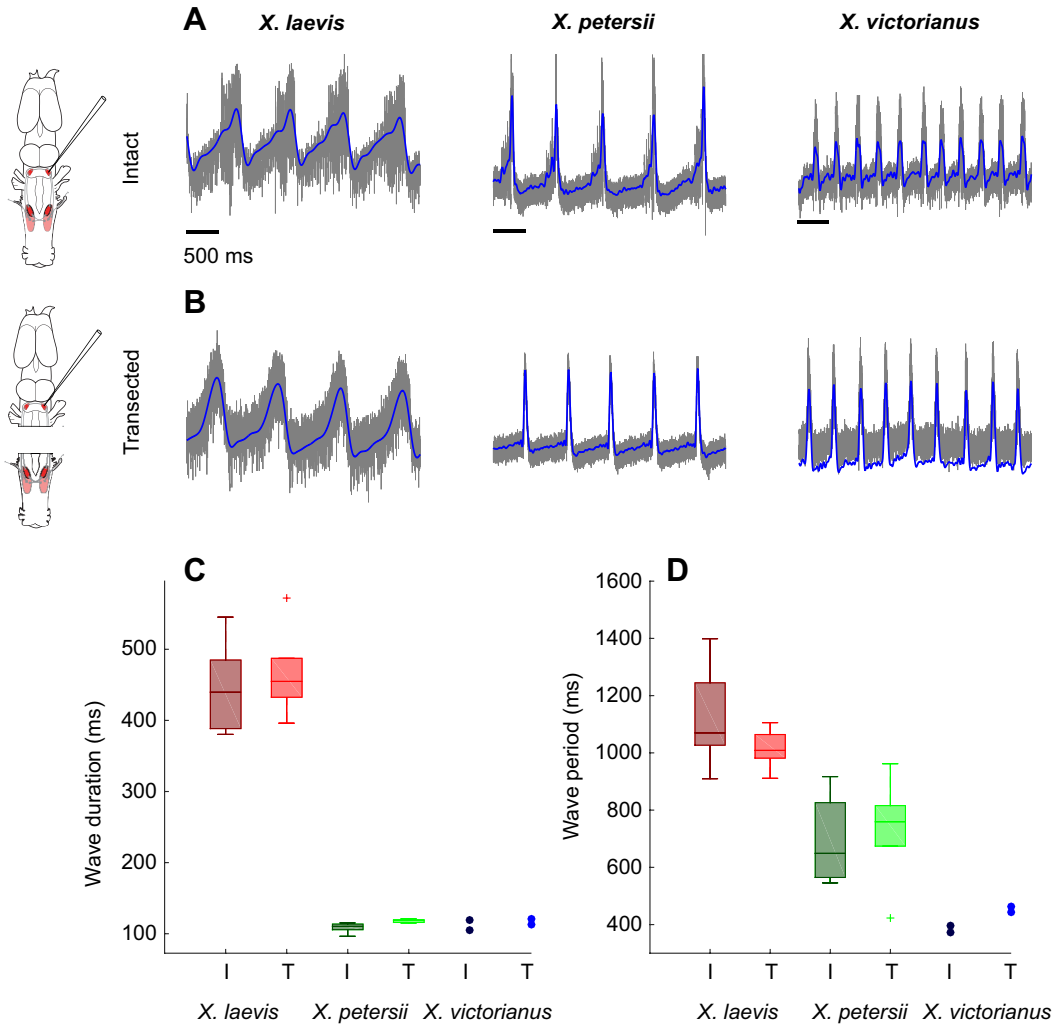

Fig. 7. Species-specific LFP wave duration and period are independent of connection to the caudal hindbrain. (A) Representative DTAM recording (gray) and LFP wave (blue) evoked by serotonin application *in vitro*. (B) Representative DTAM recording and LFP wave following transection caudal to DTAM that eliminates connections with the LMN. (C) Boxplot (as described for Fig. 2) illustrating LFP wave duration prior to [*X. laevis* (*n*=5), *X. petersii* (*n*=6) and *X. victorianus* (*n*=2)] and following caudal hindbrain transection [*X. laevis* (*n*=5), *X. petersii* (*n*=5) and *X. victorianus* (*n*=2, plotted as individual means)]. The darker shade represents intact brains (I) and the lighter shade, transected brains (T). Plus signs denote outliers. LFP wave durations are not significantly altered by transections ($P>0.05$, GLM). *Xenopus laevis* wave duration differs significantly from that of *X. petersii* and *X. victorianus* ($P<0.0001$ for each comparison, GLM). Means±s.d.: *X. laevis*: 444.2±29.6 ms intact, 465.3±28.9 ms transected; *X. petersii*: 108.7±7.3 ms intact, 118.0±2.3 ms transected; *X. victorianus*: 119.8, 105.4 ms intact, 113.2, 121.1 ms transected. (D) Boxplot illustrating LFP wave period prior to and following hindbrain transection. LFP wave periods are not significantly changed by transections ($P<0.05$, GLM). *Xenopus laevis* wave period differs significantly from that of *X. petersii* and *X. victorianus* ($P<0.0001$ for each comparison, GLM). Means±s.d.: *X. laevis*: 1115.6±188.8 ms intact, 1016.2±71.4 ms transected; *X. petersii*: 695.7±157.5 ms intact, 733.9±194.4 ms transected; *X. victorianus*: 372.9, 396.6 ms intact, 442.5, 463.3 ms transected.

activity in regulating the duration of fast trill and call periods across all three species.

Differences in DTAM LFP wave duration and period across species might be due to autonomous properties of the nucleus or instead might reflect differences in connectivity with caudal or rostral components of vocal neural circuitry. In support of the former hypothesis, we found that in all species the DTAM LFP wave persists after isolation from caudal LMN inputs. Furthermore, in *X. laevis* and *X. petersii*, the wave persists when rostral inputs from the forebrain and midbrain are also removed (*X. victorianus* was not tested). These observations suggest that species-typical characteristics of the DTAM LFP wave are intrinsic to the hindbrain compartment that includes DTAM, rather than reflecting activity elsewhere in the vocal circuit, and support an autonomous role for DTAM in control of call duration and period. Differences across species in DTAM activity could be the result of intrinsic cellular properties of DTAM neurons, network differences in synaptic connectivity within the nucleus or adjacent regions of the anterior hindbrain, or a combination of these factors.

Candidate cellular and network contributions to species-specific call duration and period

Premotor vocal neurons in DTAM

DTAM was initially identified as a target for androgens (Kelley et al., 1975; Kelley, 1980), essential hormones that support advertisement calling (Wetzel and Kelley, 1983), and as a source of input to vocal motor neurons (Wetzel et al., 1985; Zornik and Kelley 2007, 2008). More recent studies identified a population of vocal premotor neurons in *X. laevis* DTAM (fast trill neurons, FTNs) with phase-locked spikes preceding each fast trill CAP (Zornik and Yamaguchi, 2012). FTNs

Journal of Experimental Biology (2017) 220, 856-867 doi:10.1242/jeb.146845

exhibit a long-lasting depolarization (LLD) during spiking that coincides with fictive fast trill and with the DTAM LFP wave. The DTAM LFP wave thus likely reflects the activity of a population of FTNs that depolarize synchronously during fast trill. Our data suggest that a homologous population of FTNs in *X. petersii* and *X. victorianus* also generate a DTAM LFP wave by producing synchronous LLDs. However, because the waves in *X. petersii* and *X. victorianus* are shorter than those in *X. laevis*, we predict that FTN LLDs will terminate more rapidly in *X. petersii* and *X. victorianus*, leading to a brief fictive fast trill and thus a shorter call.

Intrinsic cellular contributions: ion channels and membrane properties

In *X. laevis*, intracellular recordings in synaptically isolated FTNs reveal rhythmic oscillations in response to NMDA that are similar in duration and period to LLDs recorded during fictive calling (Zornik and Yamaguchi, 2012). Intrinsic cellular properties of FTNs could thus allow them to act as network pacemakers and contribute to fast trill duration and period. For instance, *X. petersii* and *X. victorianus* FTN properties could differ from *X. laevis* FTN properties, allowing them to produce shorter oscillations.

Outward currents could contribute to call period and duration by terminating depolarization in FTNs. Candidates include: calcium-dependent potassium currents (El Manira et al., 1994; Cazalets et al., 1999; Del Negro et al., 1999; Tahvildari et al., 2008), the Na^+/K^+-ATPase hyperpolarizing current (pre-Botzinger complex; Rubin et al., 2009), A-type transient K^+ currents (lamprey locomotion: Hess and El Manira, 2001) and K^+ leak currents (respiration: Koizumi et al., 2016).

Species differences in ion channels (Harris-Warrick, 2010; Del Negro et al., 2010) expressed by FTNs could serve as control elements in species divergence of rhythmic oscillations that produce differing LLD durations in FTNs, and thus different LFP wave durations. For example, if outward current channels are more highly expressed or are activated more rapidly in *X. petersii* and *X. victorianus* than in *X. laevis*, the duration of the LLD and LFP should decrease because the neurons would be able to repolarize more rapidly. Beyond species differences in channels, differences in intracellular or extracellular regulation of Ca^{2+} levels by intracellular mechanisms or astrocytes (e.g. Morquette et al., 2015) could affect circuit properties.

Whether the intrinsic features of FTNs in *X. petersii* and *X. victorianus* can account entirely for differences in call duration and period remains to be determined. Features of network connectivity and synaptic strength might also play a role in species differences. In the stomatogastric nervous system, for example, altering synaptic strength in a reciprocally inhibitory two-cell circuit leads to large differences in burst duration and period (Sharp et al., 1996). In nematodes, differences in connectivity of homologous neurons result in distinct behaviors: *Caenorhabditis elegans* feed on bacteria using pharyngeal pumping while a related species, *Pristionchus pacificus*, uses its jaws to ingest prey. Homologous neurons produce these distinct behaviors but differ extensively in their connectivity (Bumbarger et al., 2013).

Evolution of hindbrain circuits

What is DTAM? Hindbrain circuits for respiration and vocalization

In many vocal vertebrates, respiration powers sound production, providing a potential link between hindbrain neural circuits for breathing and calling (e.g. Martin and Gans, 1972; reviewed in Leininger and Kelley, 2015). In terrestrial frogs such as *Rana*, vocalization is powered by expiration and requires activity in DTAM (aka the pretrigeminal nucleus; Schmidt, 1992, 1993). In *Xenopus*, aquatic anurans derived from terrestrial ancestors (Cannatella and de Sa, 1993; Irisarri et al., 2011), vocalization has been decoupled from respiration. Male *X. laevis* call while submerged, without respiration; glottal motor neurons that gate air movements from the lungs to the buccal cavity are inhibited during vocalization (Zornik and Kelley, 2008). A possible evolutionary scenario for the role of DTAM in vocal patterning is the repurposing of a neural circuit element, which functions during expiration in other vertebrates, to drive vocal patterning in the absence of actual breathing.

In the lamprey, a basal vertebrate, expiration is driven by the rhythm-generating paratrigeminal respiratory group (pTRG) (reviewed in Bongianni et al., 2014). The pTRG is intrinsically rhythmically active and glutamatergic, and projects to vagal motor neurons (Cinelli et al., 2013), features shared with the *Xenopus* DTAM vocal circuit (reviewed in Zornik and Kelley, 2017). Both the pTRG and DTAM are located in the rostral hindbrain compartment derived from embryonic rhombomere 1 (r1; Murakami et al., 2004; Morona and González, 2009). The several shared features described above support the homology of DTAM to the pTRG.

In mammals, however, rhythmic respiratory activity (specifically inspiration) is driven by more posterior hindbrain nuclei that include the parafacial respiratory group (pFRG) and the pre-Botzinger complex (preBotC; Thoby-Brisson et al., 2009). In the mouse, the pFRG forms in r4 and the preBotC in r7 (Tomás-Roca et al., 2016). Thus, although the lamprey pTRG has been considered a homolog of the preBotC (Cinelli et al., 2013), neither its location in r1 nor its prominent role in expiration (as opposed to inspiration, which is passive in lampreys; Bongianni et al., 2014) supports this assignment.

Is there a mammalian homolog of pTRG/DTAM that functions in expiration? The strongest candidate (Wetzel et al., 1985) is the Kolliker–Fuse nucleus of the parabrachial complex (PBC), which includes rhythmically active neurons linked to both inspiration and expiration (Dick et al., 1994). The PBC has been proposed to drive breathing patterns (Forster et al., 2014). Like neurons in DTAM and pTRG, neurons in the PBC originate in r1 (Tomás-Roca et al., 2016), are glutamatergic (Yokota et al., 2007), are rhythmic (Dick et al., 1994; Forster et al., 2014), and project to vagal and laryngeal motor neurons (nucleus ambiguus: Browaldh et al., 2015; the LMN). Thus, DTAM, pTRG and PBC are candidate vertebrate homologs. Neurons in the PBC are also active during vocalization in mammals (Farley et al., 1992; Jürgens, 2002), suggesting a highly conserved role for this hindbrain complex in both respiration and vocalization.

Evolutionary insights from comparative approaches to neural circuits

Conservation of motor patterns

As we show here for the *laevis* clade, control of duration and period of the DTAM LFP wave could provide a conserved tuning mechanism across the *Xenopus* phylogeny. For example, within a different clade, the ability of male *X. boumbaensis* to produce a single sound pulse driven by a short train of CAPs could reflect shortening of the DTAM LFP duration to produce the very short CAP train observed *in vitro* (Leininger and Kelley, 2013). The major anuran suborders include the Archaeobatrachia (e.g. *Xenopus*) and the Neobatrachia (e.g. *Rana*) (Igawa et al., 2008; Roelants and Bossuyt, 2005). A DTAM LFP has also been observed during fictive calling in *Rana pipiens* (Schmidt, 1992), suggesting an ancient (Permian/Tertiary) role for the DTAM in vocal patterning within the Anura.

Divergence of vocal patterns and auditory sensitivity during speciation

Small changes in neural circuits can cause behavior patterns to diverge so that even highly genetically similar species exhibit

distinct patterns (Katz and Harris-Warrick, 1999). Here, we identified the circuit differences underlying distinct call patterns in closely related species of *Xenopus*. Reinforcement of differences between male courtship calls has been proposed as a driver for speciation in recently diverged frog lineages (Hoskin et al., 2005). Species differences in courtship patterns enable individuals to preferentially mate with members of their own lineage and avoid the reproductive costs of hybridization (Hoskin and Higgie, 2010). Behavioral studies have shown that advertisement calls in frogs serve as a strong premating isolation mechanism; in two-choice phonotaxis experiments, females strongly prefer a conspecific advertisement call over that of another species (Gerhardt and Doherty, 1988).

Related species can exhibit behavioral and neural preferences for different call features. For instance, female *Hyla chrysoscelis* use pulse rate to recognize mates while *Hyla versicolor* females use pulse duration. These species preferences are reflected in differences in selectivity of interval-counting neurons and long-interval selective neurons in the inferior colliculus (Schul and Bush, 2002; Rose et al., 2015; Hanson et al., 2016). The *X. laevis* inferior colliculus is also populated by auditory neurons that respond preferentially to sound pulse rate (Elliott et al., 2011) and auditory sensitivity to temporal features of sound pulses could differ in *X. petersii* and *X. victorianus*.

Thus, tuning of the duration and period of premotor activity in the rhythmically active premotor hindbrain nucleus, DTAM, is a likely source of the divergence of vocal patterns in the closely related species, *X. laevis*, *X. petersii* and *X. victorianus*. This mechanism is also a candidate for the control of vocal patterns in other *Xenopus* species as well as more distantly related Anuran species. Changes in DTAM activity of related populations resulting in vocalization differences might have served as pre-zygotic barriers that prevented gene flow and thus facilitated speciation.

Acknowledgements
We thank Sarah Woolley and Dustin Rubenstein for helpful input on the project, Ben Evans for clarification of phylogenetic terminology, the National *Xenopus* Resource Center at the Marine Biological Laboratory for hosting scientific consultations, Irene Ballagh for the brain schematic diagram in Fig. 3A, Alexandro Ramirez for input on data analyses and Albyn Jones for statistical consultation.

Competing interests
The authors declare no competing or financial interests.

Author contributions
All authors contributed to the design of experiments and the analysis of the data. C.L.B. carried out the experiments and wrote the manuscript with input from D.B.K. and E.Z.

Funding
We acknowledge the support of the National Science Foundation Graduate Research Fellowship Program (C.L.B.), start-up funds from Reed College (E.Z.) and the National Institutes of Health [grant NS23684 (D.B.K.)]. Deposited in PMC for release after 12 months.

References
Albersheim-Carter, J., Blubaum, A., Ballagh, I. H., Missaghi, K., Siuda, E. R., McMurray, G., Bass, A. H., Dubuc, R., Kelley, D. B., Schmidt, M. F. et al. (2016). Testing the evolutionary conservation of vocal motoneurons in vertebrates. *Respir. Physiol. Neurobiol.* **224**, 2-10.

Bongianni, F., Mutolo, D., Cinelli, E. and Pantaleo, T. (2014). Neural mechanisms underlying respiratory rhythm generation in the lamprey. *Respir. Physiol. Neurobiol.* **224**, 1-10.

Brahic, C. J. and Kelley, D. B. (2003). Vocal circuitry in Xenopus laevis: telencephalon to laryngeal motor neurons. *J. Comp. Neurol.* **464**, 115-130.

Browaldh, N., Bautista, T. G., Dutschmann, M., and Berkowitz, R. G. (2015). The Kölliker-Fuse nucleus: a review of animal studies and the implications for cranial nerve function in humans. *Eur. Arch. Otorhinolaryngol.* **273**, 3505-3510.

Bumbarger, D. J., Riebesell, M., Rödelsperger, C. and Sommer, R. J. (2013). System-wide rewiring underlies behavioral differences in predatory and bacterial-feeding nematodes. *Cell* **152**, 109-119.

Cannatella, D. C. and de Sa, R. O. (1993). Xenopus laevis as a model organism. *Syst. Biol.* **42**, 476-507.

Cazalets, J.-R., Sqalli-Houssaini, Y. and Magoul, R. (1999). Differential effects of potassium channel blockers on the activity of the locomotor network in neonatal rat. *Brain Res.* **827**, 185-197.

Chakraborty, M. and Jarvis, E. D. (2015). Brain evolution by brain pathway duplication. *Philos. Trans. R. Soc. B Biol. Sci.* **370**, 20150056.

Cinelli, E., Robertson, B., Mutolo, D., Grillner, S., Pantaleo, T. and Bongianni, F. (2013). Neuronal mechanisms of respiratory pattern generation are evolutionary conserved. *J. Neurosci.* **33**, 9104-9112.

Del Negro, C. A., Hsiao, C. F. and Chandler, S. H. (1999). Outward currents influencing bursting dynamics in guinea pig trigeminal motoneurons. *J. Neurophysiol.* **81**, 1478-1485.

Del Negro, C. A., Hayes, J. A., Pace, R. W., Brush, B. R., Teruyama, R. and Feldman, J. L. (2010). Synaptically activated burst-generating conductances may underlie a group-pacemaker mechanism for respiratory rhythm generation in mammals. *Prog. Brain Res.* **187**, 111-136.

Dick, T. E., Bellingham, M. C. and Richter, D. W. (1994). Pontine respiratory neurons in anesthetized cats. *Brain Res.* **636**, 259-269.

El Manira, A., Tegnér, J. and Grillner, S. (1994). Calcium-dependent potassium channels play a critical role for burst termination in the locomotor network in lamprey. *J. Neurophysiol.* **72**, 1852-1861.

Elliott, T. M., Christensen-Dalsgaard, J. and Kelley, D. B. (2011). Temporally selective processing of communication signals by auditory midbrain neurons. *J. Neurophysiol.* **105**, 1620-1632.

Evans, B. J., Kelley, D. B., Tinsley, R. C., Melnick, D. J. and Cannatella, D. C. (2004). A mitochondrial DNA phylogeny of African clawed frogs: phylogeography and implications for polyploid evolution. *Mol. Phylogenet. Evol.* **33**, 197-213.

Farley, G. R., Barlow, S. M. and Netsell, R. (1992). Factors influencing neural activity in parabrachial regions during cat vocalizations. *Exp. Brain Res.* **89**, 341-351.

Forster, H., Bonis, J., Krause, K., Wenninger, J., Neumueller, S., Hodges, M. and Pan, L. (2014). Contributions of the pre-Bötzinger complex and the Kölliker-fuse nuclei to respiratory rhythm and pattern generation in awake and sleeping goats. *Prog. Brain Res.* **209**, 73-89.

Furman, B. L. S., Bewick, A. J., Harrison, T. L., Greenbaum, E., Gvoždík, V., Kusamba, C. and Evans, B. J. (2015). Pan-African phylogeography of a model organism, the African clawed frog '*Xenopus laevis*'. *Mol. Ecol.* **24**, 909-925.

Gerhardt, H. C. (1994). The evolution of vocalization in frogs and toads. *Annu. Rev. Ecol. Syst.* **25**, 293-324.

Gerhardt, H. C. and Doherty, J. A. (1988). Acoustic communication in the gray treefrog, Hyla versicolor: evolutionary and neurobiological implications. *J. Comp. Physiol. A* **162**, 261-278.

Hall, I. C., Ballagh, I. H. and Kelley, D. B. (2013). The *Xenopus* amygdala mediates socially appropriate vocal communication signals. *J. Neurosci.* **33**, 14534-14548.

Hanson, J. L., Rose, G. J., Leary, C. J., Graham, J. A., Alluri, R. K. and Vasquez-Opazo, G. A. (2016). Species specificity of temporal processing in the auditory midbrain of gray treefrogs: long-interval neurons. *J. Comp. Physiol. A Neuroethol. Sens. Neural Behav. Physiol.* **202**, 67-79.

Harris-Warrick, R. M. (2010). General principles of rhythmogenesis in central pattern generator networks. *Prog. Brain Res.* **187**, 213-222.

Hess, D. and El Manira, A. E. (2001). Characterization of a high-voltage-activated IA current with a role in spike timing and locomotor pattern generation. *Proc. Natl. Acad. Sci. USA* **98**, 5276-5281.

Hoskin, C. J. and Higgie, M. (2010). Speciation via species interactions: the divergence of mating traits within species. *Ecol. Lett.* **13**, 409-420.

Hoskin, C. J., Higgie, M., McDonald, K. R. and Moritz, C. (2005). Reinforcement drives rapid allopatric speciation. *Nature* **437**, 1353-1356.

Igawa, T., Kurabayashi, A., Usuki, C., Fujii, T. and Sumida, M. (2008). Complete mitochondrial genomes of three neobatrachian anurans: a case study of divergence time estimation using different data and calibration settings. *Gene* **407**, 116-129.

Irisarri, I., Vences, M., San Mauro, D., Glaw, F. and Zardoya, R. (2011). Reversal to air-driven sound production revealed by a molecular phylogeny of tongueless frogs, family Pipidae. *BMC Evol. Biol.* **11**, 114.

Jürgens, U. (2002). Neural pathways underlying vocal control. *Neurosci. Biobehav. Rev.* **26**, 235-258.

Katz, P. S. (2016). Evolution of central pattern generators and rhythmic behaviours. *Philos. Trans. R. Soc. B Biol. Sci.* **371**, 20150057.

Katz, P. S. and Harris-Warrick, R. M. (1999). The evolution of neuronal circuits underlying species-specific behavior. *Curr. Opin. Neurobiol.* **9**, 628-633.

Kelley, D. B. (1980). Auditory and vocal nuclei in the frog brain concentrate sex hormones. *Science* **207**, 553-555.

Kelley, D. B., Morrell, J. I. and Pfaff, D. W. (1975). Autoradiographic localization of hormone-concentrating cells in the brain of an amphibian, *Xenopus laevis*. I. Testosterone. *J. Comp. Neurol.* **164**, 47-61.

Kirkpatrick, M. and Ryan, M. J. (1991). The evolution of mating preferences and the paradox of the lek. *Nature* **350**, 33-38.
Koizumi, H., Mosher, B., Tariq, M. F., Zhang, R., Koshiya, N. and Smith, J. C. (2016). Voltage-dependent rhythmogenic property of respiratory pre-Bötzinger complex glutamatergic, Dbx1-derived, and somatostatin-expressing neuron populations revealed by graded optogenetic inhibition. *eNeuro* **3**, ENEURO.0081-16.2016.
Leininger, E. C. and Kelley, D. B. (2013). Distinct neural and neuromuscular strategies underlie independent evolution of simplified advertisement calls. *Proc. R. Soc. B Biol. Sci.* **280**, 20122639.
Leininger, E. C. and Kelley, D. B. (2015). Evolution of courtship songs in Xenopus: vocal pattern generation and sound production. *Cytogenet. Genome Res.* **145**, 302-314.
Leininger, E. C., Kitayama, K. and Kelley, D. B. (2015). Species-specific loss of sexual dimorphism in vocal effectors accompanies vocal simplification in African clawed frogs (*Xenopus*). *J. Exp. Biol.* **218**, 849-857.
Martin, W. F. and Gans, C. (1972). Muscular control of the vocal tract during release signaling in the toad Bufo valliceps. *J. Morphol.* **137**, 1-27.
Morona, R. and González, A. (2009). Immunohistochemical localization of calbindin-D28k and calretinin in the brainstem of anuran and urodele amphibians. *J. Comp. Neurol.* **515**, 503-537.
Morquette, P., Verdier, D., Kadala, A., Féthière, J., Philippe, A. G., Robitaille, R. and Kolta, A. (2015). An astrocyte-dependent mechanism for neuronal rhythmogenesis. *Nat. Neurosci.* **18**, 844-854.
Murakami, Y., Pasqualetti, M., Takio, Y., Hirano, S., Rijli, F. M. and Kuratani, S. (2004). Segmental development of reticulospinal and branchiomotor neurons in lamprey: insights into the evolution of the vertebrate hindbrain. *Development* **131**, 983-995.
Picker, M. D. (1983). Hormonal induction of the aquatic phonotactic response of Xenopus. *Behaviour* **84**, 74-90.
Rhodes, H. J., Yu, H. J. and Yamaguchi, A. (2007). Xenopus vocalizations are controlled by a sexually differentiated hindbrain central pattern generator. *J. Neurosci.* **27**, 1485-1497.
Roelants, K. and Bossuyt, F. (2005). Archaeobatrachian paraphyly and Pangaean diversification of crown-group frogs. *Syst. Biol.* **54**, 111-126.
Rose, G. J., Hanson, J. L., Leary, C. J., Graham, J. A., Alluri, R. K. and Vasquez-Opazo, G. A. (2015). Species-specificity of temporal processing in the auditory midbrain of gray treefrogs: interval-counting neurons. *J. Comp. Physiol. A* **201**, 485-503.
Rubin, J. E., Hayes, J. A., Mendenhall, J. L. and Del Negro, C. A. (2009). Calcium-activated nonspecific cation current and synaptic depression promote network-dependent burst oscillations. *Proc. Natl. Acad. Sci. USA* **106**, 2939-2944.
Ryan, M. J. and Rand, A. S. (1993). Species recognition and sexual selection as a unitary problem in animal communication. *Evolution* **47**, 647-657.
Schmidt, R. S. (1992). Neural correlates of frog calling: production by two semi-independent generators. *Behav. Brain Res.* **50**, 17-30.
Schmidt, R. S. (1993). Anuran calling circuits: inhibition of pretrigeminal nucleus by prostaglandin. *Horm. Behav.* **27**, 82-91.
Schul, J. and Bush, S. L. (2002). Non-parallel coevolution of sender and receiver in the acoustic communication system of treefrogs. *Proc. R. Soc. B Biol. Sci.* **269**, 1847-1852.
Sharp, A. A., Skinner, F. K. and Marder, E. (1996). Mechanisms of oscillation in dynamic clamp constructed two-cell half-center circuits. *J. Neurophysiol.* **76**, 867-883.
Simpson, H. B., Tobias, M. L. and Kelley, D. B. (1986). Origin and identification of fibers in the cranial nerve IX-X complex of Xenopus laevis: Lucifer Yellow backfills in vitro. *J. Comp. Neurol.* **244**, 430-444.
Tahvildari, B., Alonso, A. A. and Bourque, C. W. (2008). Ionic basis of ON and OFF Persistent Activity in Layer III Lateral Entorhinal Cortical Principal Neurons. *J. Neurophysiol.* **99**, 2006-–22011.
Thoby-Brisson, M., Karlén, M., Wu, N., Charnay, P., Champagnat, J. and Fortin, G. (2009). Genetic identification of an embryonic parafacial oscillator coupling to the preBötzinger complex. *Nat. Neurosci.* **12**, 1028-1035.
Tobias, M. and Kelley, D. (1987). Vocalizations by a sexually dimorphic isolated larynx: peripheral constraints on behavioral expression. *J. Neurosci.* **7**, 3191-3197.
Tobias, M., Evans, B. and Kelley, D. (2011). Evolution of advertisement calls in African clawed frogs. *Behaviour* **148**, 519-549.
Tomás-Roca, L., Corral-San-Miguel, R., Aroca, P., Puelles, L. and Marín, F. (2016). Crypto-rhombomeres of the mouse medulla oblongata, defined by molecular and morphological features. *Brain Struct. Func.* **221**, 815-838.
West-Eberhard, M. J. (1983). Sexual selection, social competition, and speciation. *Q. Rev. Biol.* **58**, 155-183.
Wetzel, D. M. and Kelley, D. B. (1983). Androgen and gonadotropin effects on male mate calls in South African clawed frogs, Xenopus laevis. *Horm. Behav.* **17**, 388-404.
Wetzel, D. M., Haerter, U. L. and Kelley, D. B. (1985). A proposed neural pathway for vocalization in South African clawed frogs, *Xenopus laevis*. *J. Comp. Physiol. A* **157**, 749-761.
Yager, D. D. (1992). A unique sound production mechanism in the pipid anuran *Xenopus borealis*. *Zool. J. Linn. Soc.* **104**, 351-375.
Yamaguchi, A. and Kelley, D. B. (2000). Generating sexually differentiated vocal patterns: laryngeal nerve and EMG recordings from vocalizing male and female African clawed frogs (*Xenopus laevis*). *J. Neurosci.* **20**, 1559-1567.
Yamaguchi, A., Gooler, D., Herrold, A., Patel, S. and Pong, W. W. (2008). Temperature-dependent regulation of vocal pattern generator. *J. Neurophysiol.* **100**, 3134-3143.
Yokota, S., Oka, T., Tsumori, T., Nakamura, S. and Yasui, Y. (2007). Glutamatergic neurons in the Kölliker-Fuse nucleus project to the rostral ventral respiratory group and phrenic nucleus: a combined retrograde tracing and in situ hybridization study in the rat. *Neurosci. Res.* **59**, 341-346.
Yu, H. J. and Yamaguchi, A. (2010). Endogenous serotonin acts on 5-HT2C-like receptors in key vocal areas of the brain stem to initiate vocalizations in *Xenopus laevis*. *J. Neurophysiol.* **103**, 648-658.
Zornik, E. and Kelley, D. B. (2007). Breathing and calling: neuronal networks in the Xenopus laevis hindbrain. *J. Comp. Neurol.* **501**, 303-315.
Zornik, E. and Kelley, D. B. (2008). Regulation of respiratory and vocal motor pools in the isolated brain of Xenopus laevis. *J. Neurosci.* **28**, 612-621.
Zornik, E. and Kelley, D. B. (2017). Hormones and vocal systems: insights from *Xenopus*. In *Hormones, Brain, and Behavior*, 3rd edition, Vol 2 (ed. D. W. Pfaff and M. Joëls), pp. 131–144. Oxford: Academic Press.
Zornik, E. and Yamaguchi, A. (2012). Coding rate and duration of vocalizations of the frog, Xenopus laevis. *J. Neurosci.* **32**, 12102-12114.
Zornik, E., Katzen, A. W., Rhodes, H. J. and Yamaguchi, A. (2010). NMDAR-dependent control of call duration in Xenopus laevis. *J. Neurophysiol.* **103**, 3501-3515.